Synthesis, characterization and biological activity of three square-planar complexes of Ni(II) with ethyl (2E)-2-[2-(diphenylphosphino) benzylidene]hydrazinecarboxylate and monoden...

ARTICLE *in* EUROPEAN JOURNAL OF MEDICINAL CHEMISTRY · AUGUST 2013

Impact Factor: 3.45 · DOI: 10.1016/j.ejmech.2013.07.039 · Source: PubMed

10 AUTHORS, INCLUDING:

Miroslava T Vujcic
University of Belgrade
41 PUBLICATIONS **365** CITATIONS
SEE PROFILE

Nevenka Gligorijevic
Institut za onkologiju i radiologiju Srbije
20 PUBLICATIONS **129** CITATIONS
SEE PROFILE

Katarina Jovanović
Institut za onkologiju i radiologiju Srbije
13 PUBLICATIONS **34** CITATIONS
SEE PROFILE

Sinisa Radulovic
Institut za onkologiju i radiologiju Srbije
199 PUBLICATIONS **1,845** CITATIONS
SEE PROFILE

European Journal of Medicinal Chemistry 68 (2013) 111–120

Contents lists available at ScienceDirect

European Journal of Medicinal Chemistry

journal homepage: http://www.elsevier.com/locate/ejmech

Original article

Synthesis, characterization and biological activity of three square-planar complexes of Ni(II) with ethyl (2*E*)-2-[2-(diphenylphosphino) benzylidene]hydrazinecarboxylate and monodentate pseudohalides

Milica Milenković [a], Alessia Bacchi [b], Giulia Cantoni [b], Jovana Vilipić [a], Dušan Sladić [a], Miroslava Vujčić [c], Nevenka Gligorijević [d], Katarina Jovanović [d], Siniša Radulović [d], Katarina Anđelković [a,*]

[a] Faculty of Chemistry, University of Belgrade, Studentski trg 12-16, 11000 Belgrade, Serbia
[b] Dipartimento di Chimica Generale ed Inorganica, Chimica Analitica, Chimica Fisica, University of Parma, Parco Area delle Scienze 17 A, I 43100 Parma, Italy
[c] Institute of Chemistry, Technology and Metallurgy, University of Belgrade, Njegoševa 12, P.O. Box 815, 11000 Belgrade, Serbia
[d] Institute for Oncology and Radiology of Serbia, Department of Experimental Oncology, Laboratory for Experimental Pharmacology, Pasterova 14, Belgrade, Serbia

ARTICLE INFO

Article history:
Received 9 May 2013
Received in revised form
17 July 2013
Accepted 20 July 2013
Available online 11 August 2013

Keywords:
Nickel(II) complexes
Pseudohalides
X-ray crystal structures
Antimicrobial activity
Cytotoxicity

ABSTRACT

Three square-planar complexes of nickel(II) with the tridentate condensation derivative of 2-(diphenylphosphino)benzaldehyde and ethyl carbazate, and monodentate pseudohalides, have been synthesized. Their crystal structures have been determined. All the complexes showed a significant antifungal activity, while only the azido complex displayed antibacterial activity. All the complexes were cytotoxic to a panel of six tumor cell lines, the azido complex showing a similar activity as cisplatin to leukemia cell line K562 and lower toxicity to normal MRC-5 cells than that anticancer agent. The complexes interfered with cell cycle of tumor cells and induced plasmid DNA cleavage.

1. Introduction

After the discovery that auranofin [1-(thio-κS)-β-D-glucopyranose-2,3,4,6-tetraacetato](triethylphosphine)gold (in clinical use as anti-rheumatic drug) [1] possesses anticancer properties a considerable interest has been directed towards the synthesis of metal complexes with phosphine ligands and their potential use as antitumor drugs [2–7]. For the past few years one line of our research has been directed towards the synthesis of multidentate ligands which are derivatives of 2-(diphenylphosphino)benzaldehyde and the corresponding metal complexes with the aim to study versatile coordination modes of these ligands and get information on influence of structure of the obtained complexes on biological activity. We described the synthesis, characterization and biological activity of Pt(II), Pd(II), and Ni(II) complexes with the condensation derivative of 2-(diphenylphosphino)benzaldehyde and semioxamazide. In all the complexes the ligand is coordinated as a tridentate via a PNO donor set and the fourth coordination place is occupied by chloro ligand in the case of Pd(II) and Pt(II) complexes or cyanate anion in the case of Ni(II) complex. The Pd(II) and Pt(II) complexes have a square planar geometry, whereas the geometry of the Ni(II) complex is tetrahedral. This ligand showed antibacterial and antifungal activity, which was enhanced upon complexation. There was no significant difference in activities of complexes of different metals [8]. As a continuation of this investigation we synthesized Pd(II) complex with the condensation product of 2-(diphenylphosphino)benzaldehyde and ethyl hydrazinoacetate. Square-planar surroundings of the palladium atom are formed by the bidentate PN coordination of the ligand, while the third and fourth coordination places are occupied by chloride anions. Palladium(II) complex with the condensation product of 2-(diphenylphosphino)benzaldehyde and ethyl hydrazinoacetate exhibits a similar effect to cisplatin on HeLa cells, inducing apoptosis followed by arrest of cells in S phase of cell cycle, while complexes of

* Corresponding author. Tel.: +381 11 3282 750.
E-mail address: kka@chem.bg.ac.rs (K. Anđelković).

0223-5234/$ – see front matter © 2013 Elsevier Masson SAS. All rights reserved.
http://dx.doi.org/10.1016/j.ejmech.2013.07.039

platinum(II) and palladium(II) with the condensation product of 2-(diphenylphosphino)benzaldehyde and semioxamazide induce apoptosis in HeLa cells without significant perturbations of cell cycle distribution. Complexes of platinum(II) and palladium(II) with the condensation product of 2-(diphenylphosphino)benzaldehyde and semioxamazide showed a strong cytotoxicity to CDDP-resistant U2-OS/Pt cells [9]. Recently, we described the synthesis, characterization and preliminary evaluation of the biological activity of Co(III) complex with a ligand which is the condensation derivative of 2-(diphenylphosphino)benzaldehyde and ethyl carbazate (**HL**). In the cobalt(III) complex two deprotonated ligand molecules coordinate the metal atom in a distorted octahedral geometry by chelation through the PNO donor system. The complex showed a moderate antibacterial activity and a strong cytotoxic activity, stronger than cisplatin. Cobalt(III) complex in HeLa cells induced a decrease of percentage of cells in G1 and a slight increase of percentage of cells in the S phase of cell cycle, with no important increase of apoptotic fraction of cells. The effects on cell cycle progression were temporary. Cells that survived treatment were able to recover to normal cell cycle, indicating that the investigated complex induced reversible interactions with DNA. Results of cell cycle progression, apoptotic assays, spectroscopic and electrophoretic studies showed that high cytotoxicity and moderate potential of induction of apoptosis are not a consequence of interactions with DNA [10]. As a part of our ongoing research on the coordination and biological chemistry of the condensation derivative of 2-(diphenylphosphino)benzaldehyde and ethyl carbazate here in nickel(II) complexes of the general formula [NiLX] ($X = N_3^-$, NCS^-, NCO^-) (Scheme 1. **1**–**3**) have been synthesized and their antitumor and antimicrobial activities have been evaluated.

2. Results and discussion

2.1. Synthesis

The ligand ethyl (2*E*)-2-[2-(diphenylphosphino)benzylidene] hydrazinecarboxylate (**HL**) was prepared as described previously [10]. This ligand was used for preparation of **1**, **2** and **3** complexes (Scheme 1). In these complexes ligand was coordinated in monoanionic form. Deprotonation of the ligand is facilitated by the appropriate pH of reaction medium as a result of the presence of acetate ions, basic NaOCN or NaN_3. Square-planar surroundings of the nickel atom are formed by the tridentate PNO coordination of the deprotonated enol tautomer of ligand and the coordinated monodentate cyanate, thiocyanate or azide group. Pseudohalides in the fourth coordination place were used to decrease substitution rates in this position and contribute to stabilization and biological activity of the complexes [11].

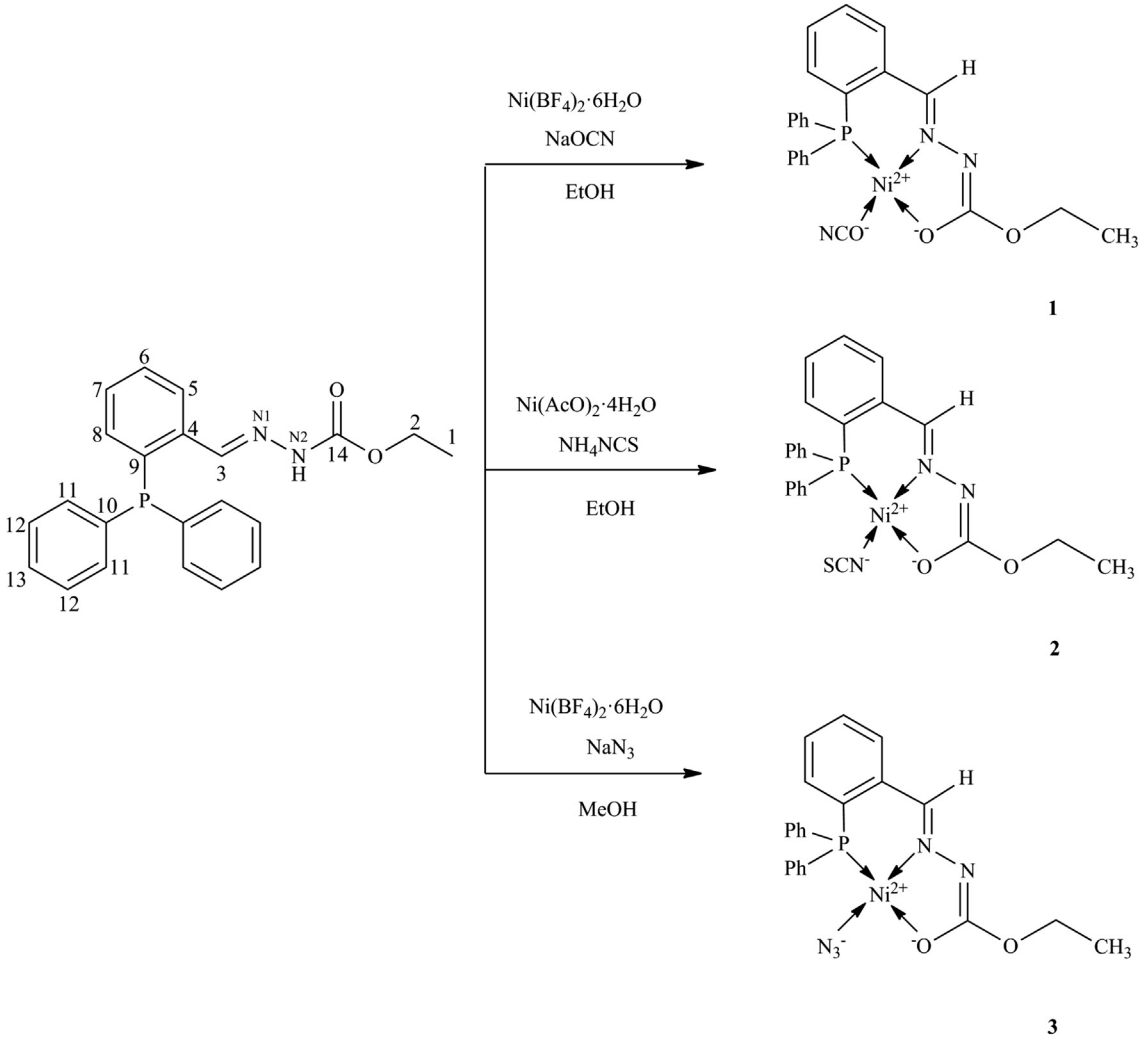

Scheme 1. Synthesis of complexes **1**–**3**.

2.2. IR spectra

Comparison of IR spectra of ligand **HL** and complexes **1**–**3** indicates the complex formation. A new band appeared in the complexes (1527 cm^{-1} for **1**, 1521 cm^{-1} for **2**, 1522 cm^{-1} for **3**), originating from $\nu(^{-}O-C{=}N)$ of the deprotonated hydrazide moiety, instead of the carbonyl band from the uncoordinated ligand at 1707 cm^{-1}. In the IR spectrum of **1** there is a band at 2219 cm^{-1} due to coordinated cyanate ion. A band at 2090 cm^{-1} in the spectrum of **2** originates from ν(CN) vibrations of NCS group coordinated via nitrogen atom. In the IR spectrum of **3** there is a band at 2038 cm^{-1} corresponding to coordinated azide ion.

2.3. NMR spectra

From the ^{1}H NMR spectra of complexes **1**–**3** (Table 1) it can be seen that the ligand is coordinated in monodeprotonated form, since the signal of hydrazide NH at 11.20 ppm is absent. In the ^{1}H NMR spectra of complexes **1**–**3** chemical shifts of most aromatic protons have higher values, due to electron withdrawal by the coordinated metal ion. The signal of CH from the hydrazone function is shifted upfield in all complexes due to coordination of the hydrazone nitrogen. The signals of the methylene and methyl groups of the alcohol part of the ester are shifted only slightly downfield in the spectra of complexes, indicating that the alkoxy oxygen was not coordinated.

From the ^{13}C NMR spectra (Table 2) it can be seen that in all complexes coordination sites are the phosphorus atom, the imine nitrogen (N1), and the carbonyl oxygen (O2). Coordination through N1 results in a downfield shift of the imine carbon C3. Due to coordination via the phosphorus atom the signals of carbon atoms directly bound to phosphorus are shifted upfield. Coordination through phosphorus atom results in electron withdrawal of aromatic carbon atoms most of which are shifted downfield. From the ^{13}C NMR spectra it can be evidenced that there is a strong downfield shift of the carbonyl carbon C14 due to coordination to Ni(II).

2.4. X-ray Crystallographic analysis

Complex **1** and **2** crystallized in a monoclinic $P2_1/n$ system, while complex **3** in a triclinic P-1 space group. In all the structures the metal center shows a square-planar geometry of coordination, where three positions are constituted by the PNO donor system formed by the phosphorus, the imine nitrogen and the carbonyl oxygen, while the fourth position is occupied by a ligand that is different for every complex: in **1** the cyanate group coordinates the metal through the oxygen atom; in **2** and **3** it is a nitrogen that is bounded to the nickel, belonging respectively to a thiocyanate and an azide group (Fig. 1).

The three complexes show a square-planar geometry slightly distorted, with the angle N1–Ni1–O1 = 83.62° (**1**), 84.17° (**2**), 83.90° (**3**) and the angle N1–Ni1–P1 = 94.45° (**1**), 95.74° (**2**), 94.09° (**3**) that are respectively part of a five- and six-membered chelation ring; the N1–N2–C8–O1–Ni1 ring is always strictly planar, while the N1–C7–C1–C2–P1–Ni1 ring shows an envelope conformation with the phosphorus at the flap, a feature common in similar systems [12–14].

Table 3 reports relevant bonding parameters for all the complexes; the bond distances and angles are very similar and they are not significantly different than the average observed for similar system, with some exceptions regarding the square planar (s.p.) Ni–L′ (L′ = cyanate, thiocyanate and azide) moiety. With regard to complex **1**, no s.p. Ni–OCN systems were found in the CSD; however, a s.p. Pt-cyanate moiety (CSD refcode BAWXEE) shows shorter O3–C23 (Δ = 0.112 Å) and longer C23–N3 (Δ = 0.044 Å) bond distances, accompanied by a larger metal–O3–C23 angle (Δ = 16.95°). The research performed for complex **2** revealed that the bond between the nickel and the nitrogen of the thiocyanate ligand results to be slightly shorter than the average value found in literature for the 85 known square planar Ni–NCS systems (average value is 1.871 Å), and the angle Ni1–N3–C23 is slightly smaller (average value is 172°). Finally we found in literature 30 Ni–N_3 moieties comparable with complex **3**: no significant differences in the bond distances were detected, while the angle Ni1–N3–N4 in complex **3** resulted to be smaller than the average (124°).

Moreover, the three square-planar complexes reported here are comparable with the one containing a similar, but neutral ligand, (2-(diphenylphosphino)benzaldehyde benzoylhydrazone-N,P)-acetyl-palladium(II) trifluoromethanesulfonate (CSD refcode BAGPAB) [15]; the PNO ligand in complex **1**, **2** and **3** shows an

Table 1
^{1}H NMR spectral data of **HL**, **1**, **2** and **3**.

Assignment	Chemical shift (ppm), multiplicity, number of H-atoms, coupling constant *J* in Hz			
	HL	**1**	**2**	**3**
C1	1.19 (t, 3H, *J* = 7.1 Hz)	1.29 (t, 3H, *J* = 7.0 Hz)	1.29 (t, 3H, *J* = 7.0 Hz)	1.31 (s, 3H)
C2	4.10 (q, 2H, *J* = 7.0 Hz)	4.22 (q, 2H, *J* = 7.0 Hz)	4.20 (q, 2H, *J* = 7.0 Hz)	4.25 (d, 4H, *J* = 6.5 Hz)
C3	8.71 (s, 1H)	7.89 (s, 1H)	7.92 (s, 1H)	7.92 (s, 1H)
C5	6.80 (m, 1H)	7.26 (m, 1H)	7.28 (m, 1H)	7.25 (d, 1H, *J* = 10 Hz)
C6	7.31 (dt, 1H, *J* = 7.5 Hz, *J* = 1 Hz)	7.38 (dt, 1H, *J* = 7.5 Hz, *J* = 0.5 Hz)	7.41 (t, 1H, *J* = 7.0 Hz)	7.36 (s, 1H)
C7	7.41 (m, 1H)	7.61 (m, 1H)	7.64 (m, 1H)	7.59 (s, 1H)
C8	7.94 (m, 1H)	7.43 (m, 1H)	7.45 (m, 1H)	7.42 (s, 1H)
C11	7.20 (m, 4H)	7.78 (t, 4H, *J* = 10.5 Hz)	7.76 (d, 4H, *J* = 6 Hz)	7.74 (s, 4H)
C12	7.41 (m, 4H)	7.52 (t, 4H, *J* = 8 Hz)	7.56 (m, 4H)	7.51(s, 4H)
C13	7.41 (m, 2H)	7.61 (m, 2H)	7.62 (m, 2H)	7.58 (s, 2H)
N2	11.20 (s, 1H)			

Table 2
^{13}C NMR spectral data of **HL**, **1**, **2** and **3**.

Assignment	^{13}C NMR chemical shift (ppm), coupling constant, *J* in Hz			
	HL	**1**	**2**	**3**
C1	14.5	14.7	14.8	14.8
C2	60.5	64.4	64.7	64.2
C3	141.6	149.1	149.5	148.8
C4	135.5 (*J* = 10 Hz)	136.1	134.3	136.4(d, *J* = 3.75 Hz)
C5	132.9	133.9	133.2	134.1
C6	129.6	130.6 (d, *J* = 4.4 Hz)	131.1	130.4
C7	129.2 (*J* = 15 Hz)	132.9	132.4	131.9
C8	125.5 (*J* = 3.75 Hz)	134.1 (d, *J* = 8 Hz)	133.5	134.0 (d, *J* = 8.12 Hz)
C9	135.6 (*J* = 18.75 Hz)	118.5 (d, *J* = 45 Hz)	118.0	118.7(d, *J* = 45.00 Hz)
C10	138.0 (*J* = 18.75 Hz)	126.4 (d, *J* = 57.5 Hz)	125.9	126.2(d, *J* = 55.00 Hz)
C11	133.5 (*J* = 20 Hz)	133.4 (d, *J* = 9.4 Hz)	133.5	133.5 (d, *J* = 9.87 Hz)
C12	128.8 (*J* = 7.5 Hz)	129.3(d, *J* = 10.25 Hz)	129.5	129.3(d, *J* = 10.25 Hz)
C13	129.1	132.1	132.4	132.8
C14	153.4	173.2	173.5	173.1
C(OCN)		135.9		
C(SCN)			134.0	

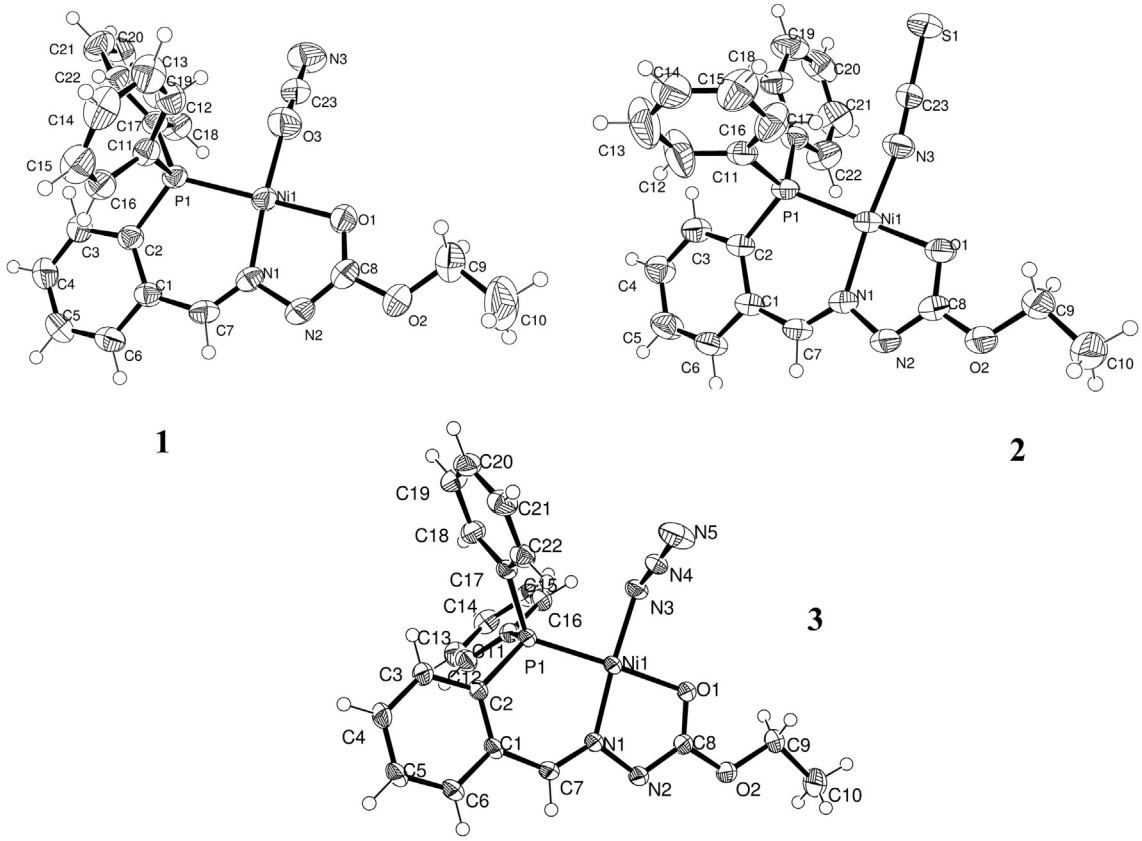

Fig. 1. Ortep diagram of complexes **1**, **2** and **3**.

elongation of the C8–O1 distance and a simultaneous shortening of the N2–C8 distance due to the deprotonation of the hydrazide; the same tendency is confirmed by comparison with the neutral free ligand, the structure of which was reported in a recent work [10].

The structure analysis of **1** does not show the presence of strong intermolecular interactions: the overall packing is governed by CH···N, CH···O and CH···C contacts. In particular the nitrogen atom of the cyanate ligand is engaged in two CH···N interactions with two molecules of complexes ($d_{C\cdots N}$ = 3.359(3) Å and $d_{C\cdots N}$ = 3.400(5) Å).

On the other hand the structure of **2** shows the formation of an interesting supramolecular motif between two adjacent molecules of complex; since the two molecules are related by a center of symmetry, the motif consists in a total of four interactions, where

Table 3
Bond lengths [Å] and angles [°] for the complexes **1**, **2** and **3**.

1		**2**		**3**	
Ni(1)–O(3)	1.851(2)	Ni(1)–N(3)	1.845(2)	Ni(1)–N(3)	1.8818(19)
Ni(1)–O(1)	1.9111(14)	Ni(1)–O(1)	1.888(1)	Ni(1)–O(1)	1.9141(15)
Ni(1)–N(1)	1.8763(16)	Ni(1)–N(1)	1.868(2)	Ni(1)–N(1)	1.8793(18)
Ni(1)–P(1)	2.1342(8)	Ni(1)–P(1)	2.1375(5)	Ni(1)–P(1)	2.1277(6)
O(3)–Ni(1)–O(1)	92.02(7)	N(3)–Ni(1)–O(1)	91.13(7)	N(3)–Ni(1)–O(1)	91.73(8)
O(3)–Ni(1)–N(1)	175.18(7)	N(3)–Ni(1)–N(1)	174.94(8)	N(1)–Ni(1)–N(3)	175.37(8)
N(1)–Ni(1)–O(1)	83.62(6)	O(1)–Ni(1)–N(1)	84.17(7)	N(1)–Ni(1)–O(1)	83.90(7)
O(3)–Ni(1)–P(1)	90.23(6)	N(3)–Ni(1)–P(1)	89.16(6)	N(3)–Ni(1)–P(1)	89.93(6)
O(1)–Ni(1)–P(1)	168.64(4)	O(1)–Ni(1)–P(1)	173.10(5)	O(1)–Ni(1)–P(1)	169.19(5)
N(1)–Ni(1)–P(1)	94.45(5)	N(1)–Ni(1)–P(1)	95.74(5)	N(1)–Ni(1)–P(1)	94.09(6)
C(17)–P(1)–C(11)	106.20(7)	C(17)–P(1)–C(11)	108.01(8)	C(17)–P(1)–C(11)	105.83(10)
C(2)–P(1)–C(17)	104.68(8)	C(17)–P(1)–C(2)	106.10(9)	C(2)–P(1)–C(17)	105.53(10)
C(2)–P(1)–C(11)	104.81(8)	C(11)–P(1)–C(2)	106.55(9)	C(2)–P(1)–C(11)	105.60(10)
C(17)–P(1)–Ni(1)	120.49(6)	C(17)–P(1)–Ni(1)	113.70(6)	C(17)–P(1)–Ni(1)	120.44(7)
C(11)–P(1)–Ni(1)	106.43(6)	C(11)–P(1)–Ni(1)	109.21(7)	C(11)–P(1)–Ni(1)	105.30(7)
C(2)–P(1)–Ni(1)	113.04(6)	C(2)–P(1)–Ni(1)	112.92(6)	C(2)–P(1)–Ni(1)	113.02(7)
C(8)–O(1)–Ni(1)	107.84(11)	C(8)–O(1)–Ni(1)	108.5(1)	C(8)–O(1)–Ni(1)	107.98(13)
C(8)–O(2)–C(9)	118.49(17)	C(8)–O(2)–C(9)	115.9(2)	C(8)–O(2)–C(9)	117.69(18)
C(7)–N(1)–N(2)	113.11(14)	C(7)–N(1)–N(2)	113.4(1)	C(7)–N(1)–N(2)	113.47(18)
C(7)–N(1)–Ni(1)	133.64(12)	C(7)–N(1)–Ni(1)	133.3(1)	C(7)–N(1)–Ni(1)	133.47(16)
N(2)–N(1)–Ni(1)	113.24(11)	N(2)–N(1)–Ni(1)	113.2(1)	N(2)–N(1)–Ni(1)	113.05(13)
C(8)–N(2)–N(1)	108.44(14)	C(8)–N(2)–N(1)	107.9(1)	C(8)–N(2)–N(1)	108.73(18)
C(23)–O(3)–Ni(1)	147.6(2)	C(23)–N(3)–Ni(1)	169.4(2)	N(4)–N(3)–Ni(1)	120.42(17)

the contacts C6–H···O2 ($d_{C\cdots O}$ = 3.372(2) Å) and C7–H···N2 ($d_{C\cdots N}$ = 3.669(2) Å) are twice repeated (Fig. 2).

Two CH···S interactions ($d_{C\cdots S}$ = 3.850(3) Å and $d_{C\cdots S}$ = 3.547(3) Å) involve the terminal sulfur atom of the isothiocyanate ligand with the aromatic ring of two different molecules of complex; an analogous contact is found between the carbonylic oxygen bound to the nickel atom and an aromatic CH ($d_{C\cdots O}$ = 3.317(2) Å).

Complex **3** crystallized as a methanol solvate form with a ratio complex:MeOH = 1:1.5; one of the two solvent molecules has the methyl group coinciding with a center of symmetry, that generates two hydroxyl groups with an occupancy = 0.5.

The methanol molecules are responsible for two hydrogen bonds (Fig. 3): the first one involves the OH group of the fully occupied methanol molecule and the amide nitrogen of the complex: O3–H3···N2 (O3···N2 = 2.869(4) Å, 166.2(3)°); while the second one concerns the partially occupied O100 oxygen atom, that alternatively contacts the O3 atom of two different methanol molecules: O100–H100···O3 (O3···O6 = 2.70(1) Å, 147(5)°).

The total packing depicted in Fig. 4 shows that the solvent molecules are placed within channels that are generated by the complex units; at room temperature crystals of **3** are not air stable: this is probably due to the tendency of the methanol molecules to exit from the structure.

2.5. Biological activity

2.5.1. Antifungal activity

Antifungal activity was evaluated against eight fungal species using disc diffusion method. The results are presented in Table 4. The ligand and all the complexes showed a significant activity at 100 μg/discs against both yeast species, *Candida albicans* and *Saccharomyces cerevisiae*, the complexes being more active. Antifungal effects of the complexes to *C. albicans* were more pronounced than either the nickel salt or salts containing the corresponding anionic ligand. The complexes and the ligand were also active to some plant pathogenic fungi. It should be born in mind that zone diameter depends on diffusion in agar, and that the complexes have low water solubility, indicating that the antifungal effects are much more pronounced than those of rapidly diffusing water-soluble salts. On the other hand, the data indicate the possibility that a part of the activity might be ascribed to transport of active anions through cell membranes, i.e. the neutral lipophilic complex can easily cross the membrane, and within the cell the relatively weakly bound monodentate anion could be released. Such a mechanism might apply for the azido complex (**3**), but is less likely for the cyanato (**1**), and thiocyanato (**2**) complexes, since the corresponding salts showed no activity against most tested strains.

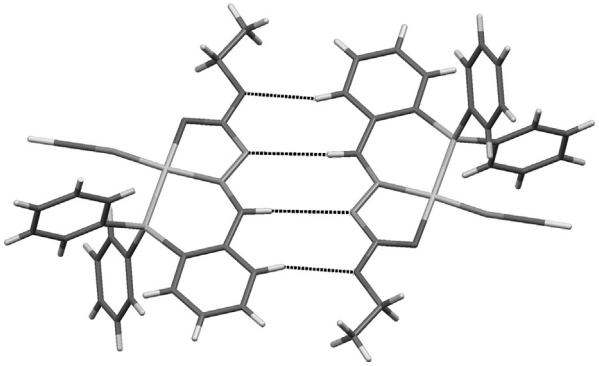

Fig. 2. Interactions between two adjacent molecules of complex **2**.

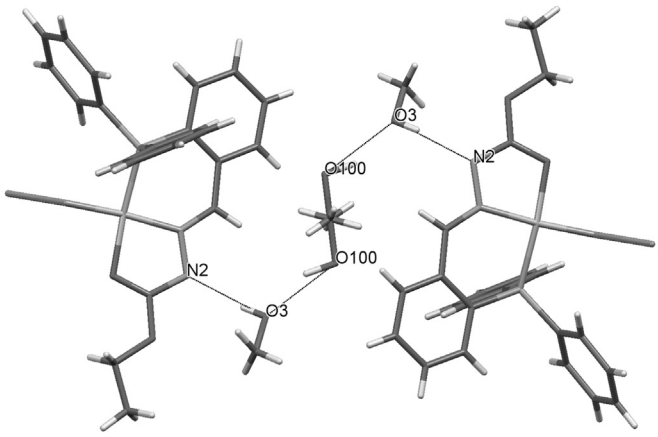

Fig. 3. Hydrogen bonds involving the methanol molecules in complex **3**.

2.5.2. Antibacterial activity

Antibacterial activity was tested against seven strains of Gram-positive and five strains of Gram-negative bacteria using disc-diffusion method. The results are given in Table 5. Contrary to antifungal effects, the antibacterial activity was poor, the ligand and two complexes being inactive, while the activity of the azido complex was lower than the activity of the nickel salt.

2.5.3. The brine shrimp test

The biological activity of the compounds **HL**, **1**, **2**, **3** was tested by the brine shrimp test (toxicity to *Artemia salina*). The results of this test can be extrapolated to cell-line toxicity and anti-tumor activity [16,17]. Results are shown in Table 6 in terms of LC_{50}. There is a significant difference in activity of three complexes, the most active complex **3**, being almost 60 times more active than the least active complex **2**.

2.5.4. MTT assay

Cytotoxic activity of the investigated nickel complexes **1**–**3**, the appropriate ligand, and nickel salt was determined by MTT assay after 48 h treatment of six tumor cell lines (A549, MDA-MB-361, HeLa, FemX, LS-174 and K562) and one normal cell line (MRC-5). Results are shown in Table 7 in terms of IC50 values, that are determined from cell survival diagrams. Values of IC50 represent

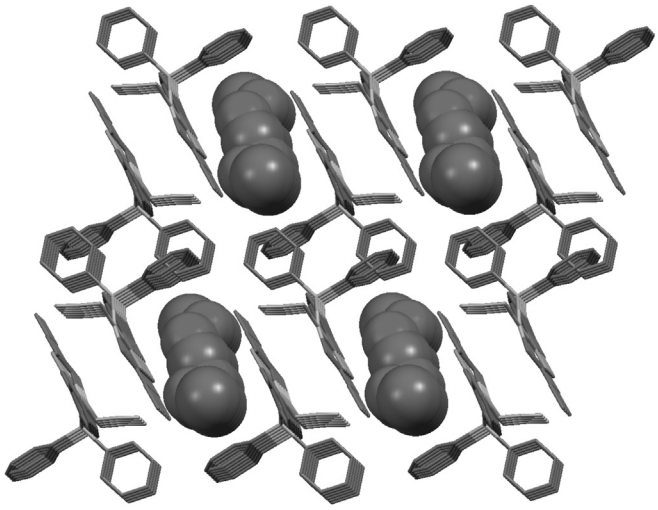

Fig. 4. The overall packing of complex **3**.

Table 4
In vitro antifungal activity (mm) of compounds (concentrations 100 μg/disc).

	F. semitectum	*F. tricinctum*	*C. albicans*	*S. cerevisiae*	*F. equiseti*	*T. viride*	*F. proliferatum*	*Penicillium* sp.
HL	–	9	9	9	–	10	–	–
1	–	–	10	10	12	12	–	–
2	–	9	11	10	–	12	–	–
3	–	10	11	9	–	10	–	28
$Ni(BF_4)_2{\cdot}6H_2O$	–	–	9	10	12	9	–	–
NaOCN	–	–	–	–	–	–	–	10
NH_4SCN	–	–	9	–	–	–	–	16
NaN_3	–	9	10	9	22	12	–	26
Nystatin[a]	28	80	30	54	80	38	30	38

– Not active.
[a] Concentration 30 μg/disc.

the average of two to three experiments, with each experiment performed in three replicates.

The ligand showed a moderate activity only to two cell lines. All the complexes showed activity to all cell lines and were more active than the ligand. It should be pointed out that the azido complex **3** showed similar activity to K562 leukemia cells as cisplatin. It is also worth mentioning that complex **3** had approximately four times higher cytotoxicity to K562 cell line than to normal MRC-5 cells, contrary to cisplatin which was similarly cytotoxic to both cell lines. All the complexes were more cytotoxic to K562 cells than to other cell lines. Among the complexes **3** was the most cytotoxic to K562 and MDA-MB-361 cells, **2** for LS-174 cell line, and **1** for normal MRC-5 cells, while for the other cell lines no significant difference could be seen.

2.5.5. Cell cycle analysis

Cell cycle analysis of HeLa cells treated with investigated nickel complexes and cisplatin was performed by flow cytometry after staining with propidium iodide [18]. Cells were continually exposed to investigated complexes for 48 h with increasing concentrations of agents (0.5× IC_{50}, IC_{50} and 1.5× IC_{50}).

Results are presented in Fig. 5 and show that all investigated complexes already at the lowest concentration corresponding to 0.5× IC_{50} induced perturbations of cell cycle. Perturbations were more pronounced as concentrations of the agents increased. Reference compound, cisplatin, in accordance with previously published data [9] induced increase of the percentage of cells in sub-G1 phase, decrease of percent of cells in G1 and G2 phase and arrest of the cell cycle in the S phase. All investigated nickel complexes induced increase of percentage of cells in sub-G1 phase and decrease of percentage of cells in G1 phase compared to control. Complexes **2** and **3** induced increase in the percent of cells in the S and G2 phase only at the highest concentration (1.5× IC_{50}).

2.5.6. DNA cleavage

The abilities of complexes **1**, **2** and **3** to cleave double-stranded plasmid DNA were investigated using an agarose gel electrophoretic assay. The assay allows assessment of DNA strand cleavage by monitoring the conversion of untreated supercoiled form (F I) plasmid DNA into the nicked form (F II) and linear form (F III). As it shown in Fig. 6 (lane P), plasmid pUC19 consisted mainly of F I. Upon the addition of complex **1** to the plasmid, the supercoiled DNA was converted into circular FII and linear FIII forms in the concentration dependent way (Fig. 6a, lanes 1–5). The generation of the linear form increased gradually up to 2 mM of **1** (lane 4), when the bands of the supercoiled and linear forms smeared. Finally band smearing appeared at maximal performed concentration of 3 mM (lane 5), indicating that complex **1** possesses a nuclease activity, converting DNA to shorter fragments. The compound **3** had a weaker nuclease activity (Fig. 6b, lanes 6–10) than **1**. The maximal cleavage effect was produced by 3 mM of the complex (lane 10). The complex **2** showed the largest activity. Already with 0.5 mM concentration of the complex **2** the plasmid DNA was converted into linear form FIII (lane 11), and with increasing concentration up to 2 mM, gradually bands smearing occurred (lanes 12–14), and at the highest concentration of 3 mM (lane 15), almost the total quantity of plasmid DNA was destroyed. These results indicate that DNA damage is, at least in part, responsible for the activity of the complexes.

3. Conclusion

The synthesized square-planar nickel(II) complexes had a common tridentate ligand, but differed in the fourth, pseudohalide anion (azide, cyanate and thiocyanate). All the complexes showed a significant antifungal activity, generally stronger than the ligand. The non-electrolyte nature of the complexes might facilitate transport of nickel and pseudohalides through biological membranes. Only the azido complex **3** had an antibacterial activity. All the complexes had a cytotoxic activity to all the tested cell lines, with all of them having preference to leukemia cell line K562. Especially strong activity to this cell line was shown by azido complex **3**, the activity of which was similar to cisplatin. Of particular interest is the fact that the activity of **3** to K562 cells was much stronger than cytotoxicity to MRC-5 normal cell line, while there was no difference in toxicity of cisplatin to these two cell

Table 5
In vitro antibacterial activity (mm) of compounds (concentrations 1 mg/disc).

	S. aureus	*M. flavus*	*S. longisporum*	*M. luteus*	*C. sporogenes*	*S. lutea*	*B. subtilis*	*E. coli*	*S. enteritidis*	*P. vulgaris*	*P. aeruginosa*	*K. pneumoniae*
HL	–	–	–	–	–	–	–	–	–	–	–	–
1	–	–	–	–	–	–	–	–	–	–	–	–
2	–	–	–	–	–	–	–	–	–	–	–	–
3	–	9	9	9	9	9	–	9	10	9	9	10
$Ni(BF_4)_2{\cdot}6H_2O$	18	14	14	14	14	14	–	16	14	16	12	14
Tetracycline[a]	24	27	24	25	24	23	25	26	25	26	25	23

– Not active.
[a] concentration 30 μg/disc.

Table 6
Toxic effect (expressed as LC_{50} values in mM) of compounds on *A. salina*.

Compound	LC_{50} (mg/disc)
HL	0.55 ± 0.05
1	0.08 ± 0.01
2	0.81 ± 0.05
3	0.014 ± 0.001
$Ni(BF_4)_2 \cdot 6H_2O$	0.12 ± 0.01

lines. The activity of all the complexes was at least in part based upon influence on cell cycle distribution (increase of percentage of cells in sub-G1 phase and decrease of percentage of cells in G1 phase) and DNA damage.

4. Experimental

4.1. Material and methods

2-(Diphenylphosphino)benzaldehyde (97%) and ethyl carbazate (97%) were obtained from Aldrich. The ligand was obtained by condensation of 2-(diphenylphosphino)benzaldehyde and ethyl carbazate using a previously described method [10]. IR spectra were recorded on a Perkin–Elmer FT-IR 1725X spectrometer using the ATR technique in the region 4000–400 cm^{-1}. ^1H NMR (500 MHz), ^{13}C NMR (125 MHz) and 2D NMR spectra were recorded on a Bruker Avance 500 spectrometer in $CDCl_3$ using TMS as internal standard for ^1H and ^{13}C. All spectra were measured at 25 °C. Nickel(II) complexes **1**–**3** were characterized on the basis of NMR spectroscopy results: 1D (^1H, ^{13}C, DEPT), 2D (COSY, NOESY) as well as 2D ^1H–^{13}C heteronuclear correlation spectra (HSQC). Elemental analyses (C, H, and N) were performed by standard micro-methods using the ELEMENTARVario ELIII C.H.N.S.O analyzer.

4.1.1. Synthesis of (*1*)

A mixture of 0.09 g (0.26 mmol) $Ni(BF_4)_2 \cdot 6H_2O$ and 0.10 g (0.26 mmol) of the ligand was dissolved in 20 mL ethanol and then 0.02 g (0.30 mmol) NaOCN was added to it. The mixture was heated at 56 °C for 2 h. The color of the solution changed from brown to orange-reddish. The reaction solution was left to stand at room temperature while the orange-reddish crystals arose from the solution. Yield 0.060 g (48.5%). IR (vs – very strong, s – strong, m – medium, w – weak): 3550 (w), 3052 (w), 3006 (w), 2219 (vs), 1555 (w), 1527 (vs), 1474 (m), 1417 (s), 1376 (m), 1331 (vs), 1170 (w), 1098 (m), 1010 (s), 879 (w), 760 (m), 700 (m). Elemental analysis calcd for $C_{23}H_{20}N_3O_3PNi$: N 8.83%, C 58.02%, H 4.23%, found: N 8.89%, C 57.95%, H 4.26%.

4.1.2. Synthesis of (*2*)

Into the mixture of 0.07 g (0.28 mmol) $Ni(AcO)_2 \cdot 4H_2O$ and 0.10 g (0.27 mmol) of the ligand in 30 mL ethanol 0.10 g (1.30 mmol) NH_4NCS was added. The mixture was heated at 65 °C for 2 h. The color of the solution changed from brown to orange-reddish. The reaction solution was left to stand at room temperature while the orange-reddish crystals arose from the solution. Yield 0.080 g (60.2%). IR (vs – very strong, s – strong, m – medium, w – weak): 3055 (w), 2982 (w), 2090 (vs), 2017 (w), 1521 (vs), 1479 (m), 1429 (vs), 1375 (s), 1337 (vs), 1099 (m), 1003 (s), 884 (w), 748 (m), 698 (w). Elemental analysis calcd for $C_{23}H_{20}N_3O_2PSNi$: N 8.54%, C 56.13%, H 4.10%, S 6.52%, found: N 8.52%, C 56.07%, H 3.89%, S 6.33%.

4.1.3. Synthesis of (*3*)

A mixture of 0.12 g (0.35 mmol) $Ni(BF_4)_2 \cdot 6H_2O$ and 0.13 g (0.35 mmol) of the ligand was dissolved in 50 mL methanol and then 0.10 g (1.54 mmol) NaN_3 was added to it. The mixture was heated at 52 °C for 2 h. The color of the solution changed from brown to purple-reddish. The purple-reddish crystals arose from the reaction solution at room temperature. Crystals are not stable in the air. Yield 0.090 g (54.3%). IR (vs – very strong, s – strong, m – medium, w – weak): 3297 (w), 3052 (w), 2986 (w), 2914 (w), 2037 (vs), 1989 (w), 1522 (vs), 1476 (s), 1421 (vs), 1386 (s), 1332 (vs), 1278 (m), 1187 (w), 1134 (w), 1096 (w), 1014 (s), 938 (w), 896 (w), 778 (w), 748 (m), 694 (m). Elemental analysis calcd for $C_{22}H_{20}N_5O_2PNi$: N 14.71%, C 55.50%, H 4.23%, found: N 14.71%, C 55.43%, H 4.08%.

4.2. Crystallographic structure determination

Single crystal X-ray diffraction data for the complexes were collected using the Mo Kα radiation (λ = 0.71073 Å) on a SMART APEX2 (**1** and **3**) and a SMART BREEZE (**2**) diffractometer; the diffraction experiment was performed at room temperature (293 K) for **1** and **2**, while for **3** at 170 K in order to prevent decay. Lorentz, polarization, and absorption corrections were applied [19]. Structures were solved by direct methods using SIR97 [20] and refined by full-matrix least-squares on all F^2 using SHELXL97 [21] implemented in the WinGX package [22]. Hydrogen atoms were introduced in calculated positions; anisotropic displacement parameters were refined for all non-hydrogen atoms.

Hydrogen bonds have been analyzed with SHELXL97 [21] and PARST97 [22] and extensive use was made of the Cambridge Crystallographic Data Centre packages [23] for the analysis of crystal packing. Table 8 summarizes crystal data and structure determination results.

Crystallographic data (excluding structure factors) for **1**, **2** and **3** have been deposited with the Cambridge Crystallographic Data Centre as supplementary publication no. CCDC 937298–937300. Copies of the data can be obtained free of charge on application to CCDC, 12 Union Road, Cambridge CB2 1EZ, UK (fax: (+44) 1223-336-033; e-mail: deposit@ccdc.cam.ac.uk).

4.3. Biological activity

4.3.1. Antifungal activity

The fungi tested were yeasts *C. albicans* (ATCC 10231) and *S. cerevisiae* (ATCC 9763) and six plant pathogenic fungi isolated from

Table 7
Results of MTT assay after 48 h continual action.

IC_{50} (μM)							
	A549	MDA-MB-361	K562	HeLa	FemX	LS-174	MRC-5
HL	>100	>100	41.8 ± 3.7	58.3 ± 0.2	>100	>100	>100
1	43.7 ± 3.3	76.2 ± 5.5	25.0 ± 0.9	31.4 ± 3.3	41.8 ± 4.8	93.3 ± 3.8	32.2 ± 5.6
2	56.1 ± 3.3	79.4 ± 8.3	29.9 ± 1.8	43.6 ± 1.9	40.5 ± 2.0	71.8 ± 0.7	62.0 ± 5.9
3	45.2 ± 0.9	38.8 ± 3.7	14.4 ± 3.7	35.5 ± 2.5	34.5 ± 8.1	78.1 ± 0.3	55.5 ± 2.4
$Ni(BF_4)_2 \cdot 6H_2O$	77.6 ± 8.6	97.4 ± 2.3	90.2 ± 3.3	>100	>100	>100	>100
CDDP	17.2 ± 0.7	14.7 ± 1.2	13.0 ± 1.8	7.8 ± 2.3	10.8 ± 0.9	22.4 ± 7.2	14.2 ± 2.8

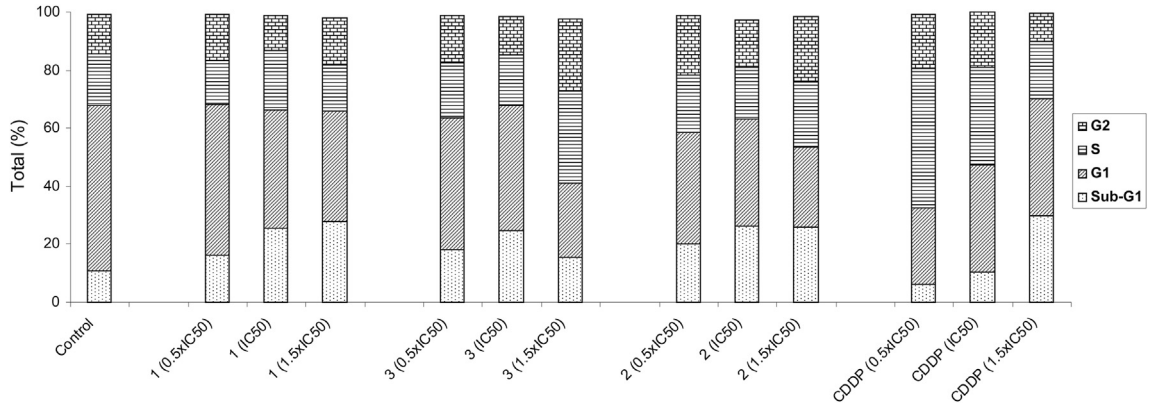

Fig. 5. Cell cycle distribution of HeLa cells after 48 h treatment with investigated nickel complexes and CDDP.

the herbal drugs provided by courtesy of Institute of Medicinal Plant Research "Dr Josif Pančić" (Belgrade, Serbia): *Trichoderma viride*, *Penicillium* sp. (both isolated from *Calendulae* flos), *Fusarium semitectum* (isolated from *Maydis* stigma), *Fusarium proliferatum* (isolated from *Calendulae* flos), *Fusarium equiseti* (isolated from *Equiseti* herba) and *Fusarium tricinctum* (isolated from *Menthae* folium and herba).

Sabouraud dextrose agar (Institute of Virology, Vaccines and Sera 'Torlak') was prepared according to the manufacturer's instructions. In each sterile Petri dish (90 mm diameter) 22 mL of previously prepared agar suspension was poured and 100 μL of fungi was added.

The substances **HL**, **1**, **2** and **3** were dissolved in DMSO and $Ni(BF_4)_2 \cdot 6H_2O$ was dissolved in water. Solutions of the compounds 10 μL (100 μg of compound per disc), were applied on filter paper discs (8 mm diameter) and the solvent was evaporated. Paper discs were placed on the agar with the fungi. Petri dishes were incubated for 48 h at 28 °C. Water solutions of NaOCN, NH_4SCN and NaN_3 were applied on filter paper discs at concentration 8.8 μg of OCN^- per disc; 11.8 μg of SCN^- per disc; 8.8 μg of N_3^- per disc, the solvent was evaporated, and the discs were placed on the agar under the same conditions as the investigated compounds.

Nystatin (Hemofarm, 30 mg of the active substance, a disc diameter of 8 mm) was used as a positive control, while the disc with 10 μL of DMSO was used as a negative test. Zone of inhibition was measured in millimeters, including the disc [24,25].

4.3.2. Antibacterial activity

The antibacterial activity was evaluated using seven different strains of the Gram-positive bacteria: *Staphylococcus aureus* (ATCC 6538), *Micrococcus flavus* (ATCC 10240), *Streptosporangium longisporum* (ATCC 25212), *Micrococcus luteus* (ATCC 4698), *Clostridium sporogenes* (ATCC 19404), *Sarcina lutea* (ATCC 9341), *Bacillus subtilis* (ATCC 6633), and five different strains of the Gram-negative bacteria: *Escherichia coli* (ATCC 25922), *Salmonella enteritidis* (ATCC 13076), *Proteus vulgaris* (ATCC 13315), *Pseudomonas aeruginosa* (ATCC 9027) and *Klebsiella pneumoniae* (ATCC 10031). A disc-diffusion method, according to the NCCLS, was employed for the determination of the antibacterial activity of the compounds [24]. All tests were performed in Nutritent agar (HiMedia). In each sterile Petri dish (90 mm diameter) 22 mL of Nutritent agar and 100 μL of bacterial suspension were added. The substances **HL**, **1**, **2** and **3** were dissolved in DMSO (1 mg/100 μL) and then 100 μL of solution was applied to filter paper discs (8 mm in diameter) and the solvent was evaporated. The nickel salt $Ni(BF_4)_2 \cdot 6H_2O$ was dissolved in water and in the amount of 1 mg applied on filter paper disc. Tetracycline (Institute of Virology, Vaccines and Sera 'Torlak') 30 μg per filter paper disc (8 mm in diameter) was used as a positive control, while the discs of the same diameter impregnated with 100 μL of DMSO were used as a negative test. Filter paper discs with the investigated compounds were placed on the agar. Petri dishes were incubated for 24 h at 37 °C. Zone of inhibition was measured in millimeters, including the disc.

4.3.3. The brine shrimp test

A teaspoon of lyophilized eggs of the brine shrimp *A. salina* was added to 0.5 L of the artificial sea water containing several drops of yeast suspension (3 mg of dry yeast in 5 mL distilled water), and air was passed through the suspension thermostated at 18–20 °C,

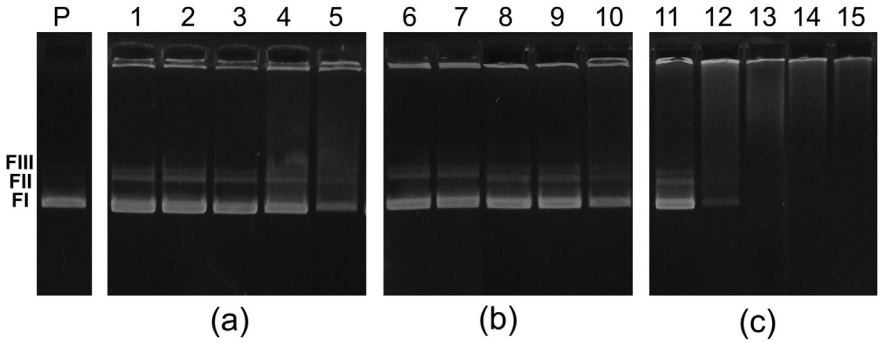

Fig. 6. Agarose gel electrophoretic analysis of cleavage plasmid pUC19 DNA in TS buffer by Ni(II) complexes: (a) **1** – lanes 1, 2, 3, 4 and 5 at 0.5 mM, 1 mM, 1.5 mM, 2 mM and 3 mM concentration, respectively; (b) **3** – lanes 6, 7, 8, 9 and 10 at 0.5 mM, 1 mM, 1.5 mM, 2 mM and 3 mM concentration, respectively; (c) **2** – lanes 11, 12, 13, 14 and 15 at 0.5 mM, 1 mM, 1.5 mM, 2 mM and 3 mM concentration, respectively; P – control pUC19 DNA.

Table 8
Crystal data and structure refinement for complexes **1**, **2** and **3**.

	1	**2**	**3**
Empirical formula	$C_{23}H_{20}N_3NiO_3P$	$C_{23}H_{20}N_3NiO_2PS$	$C_{23.5}H_{26}N_5NiO_{3.5}P$
Formula weight	476.08	492.16	524.16
Temperature	293(2) K	293(2) K	293(2) K
Wavelength	0.71073 Å	0.71073 Å	0.71073 Å
Crystal system, space group	Monoclinic, $P2_1/n$	Monoclinic, $P2_1/n$	Triclinic, P-1
Unit cell dimensions	$a = 10.529(5)$ Å $b = 13.797(5)$ Å $\beta = 97.052(5)^\circ$ $c = 14.945(5)$ Å	$a = 9.689(1)$ Å $b = 13.242(2)$ Å $\beta = 104.725(2)^\circ$ $c = 17.966(2)$ Å	$a = 10.295(1)$ Å $\alpha = 72.20(3)^\circ$ $b = 10.715(2)$ Å $\beta = 71.19(3)^\circ$ $c = 12.555(1)$ Å $\gamma = 75.13(2)^\circ$
Volume	2154.6(15) Å^3	2229.4(5) Å^3	1228.9(9) Å^3
Z	4	4	2
Calculated density	1.468 Mg/m^3	1.466 Mg/m^3	1.417 Mg/m^3
Absorption coefficient	1.005 mm^{-1}	1.061 mm^{-1}	0.892 mm^{-1}
$F(000)$	984	1016	546
Crystal size	0.09 × 0.07 × 0.05 mm	0.09 × 0.07 × 0.04 mm	0.09 × 0.07 × 0.06 mm
θ range for data collection	2.02–29.25°	1.93–32.24°	1.77–31.68°
Reflections collected/unique	31451/5855 [R(int) = 0.0307]	35850/7397 [R(int) = 0.0287]	18770/7635 [R(int) = 0.0372]
Refinement method	Full-matrix least-squares on F^2	Full-matrix least-squares on F^2	Full-matrix least-squares on F^2
Data/restraints/parameters	5855/0/280	7397/0/280	7635/9/330
Goodness-of-fit on F^2	1.038	0.764	0.813
Final R indices [$I > 2\sigma(I)$]	$R_1 = 0.0348$, $wR_2 = 0.1019$	$R_1 = 0.0377$, $wR_2 = 0.1474$	$R_1 = 0.0432$, $wR_2 = 0.1171$
R indices (all data)	$R_1 = 0.0407$, $wR_2 = 0.1069$	$R_1 = 0.0524$, $wR_2 = 0.1840$	$R_1 = 0.0676$, $wR_2 = 0.1389$
Largest ΔF maximum/minimum	0.585 and −0.635 Å^{-3}	0.631 and −0.453 e Å^{-3}	0.696 and −0.843 Å^{-3}

under illumination for 48 h. Hatched nauplii were used in further experiments.

The compounds **HL**, **1**, **2** and **3** were dissolved in DMSO and $Ni(BF_4)_2 \cdot 6H_2O$ was dissolved in water, then in various amounts (1 mg–0.0125 mg) applied to filter paper discs (8 mm in diameter) and the solvent was evaporated. Paper discs were placed on the bottom of the glass vial into which was added 1 mL of artificial sea water, and about 15–20 hatched nauplii.

The vials were left at room temperature under illumination for 24 h, and afterward live and dead nauplii were counted. All samples were done in triplicate. LC_{50} was defined as the concentration of substances that causes death of 50% nauplii.

4.3.4. Cytotoxic activity

4.3.4.1. Cell culture. Human lung adenocarcinoma epithelial cells (A549), human breast cancer cells (MDA-MB-361), human cervix carcinoma cells (HeLa), human melanoma cells (FemX), human colon cancer cells (LS-174) and human fetal lung fibroblast cells (MRC-5) were maintained as monolayer culture in nutrient medium (RPMI 1640), while human myelogenous leukemia cells (K562) were maintained in suspension culture. Powdered RPMI 1640 medium was purchased from Sigma Aldrich Co. Nutrient medium RPMI 1640 was prepared in sterile ionized water, supplemented with penicillin (192 IU/mL), streptomycin (200 μg/mL), 4-(2-hydroxyethyl)piperazine-1-ethanesulfonic acid (HEPES) (25 mM), L-glutamine (3 mM) and 10% of heat-inactivated fetal calf serum (FCS) (pH 7.2). The cells were grown at 37 °C in 5% CO_2 and humidified air atmosphere, by twice weekly subculture.

4.3.4.2. MTT assay. Cytotoxicity of the investigated nickel complexes (**1**–**3**), the appropriate triphenylphosphine ligand (**HL**), and nickel salt in comparison to cisplatin, was determined using the 3-(4,5-dimethylthiazol-2yl)-2,5-diphenyltetrazolium bromide (MTT, Sigma–Aldrich) assay [26]. Cells were seeded in 96-well cell culture plates (NUNC) A549 (5000 c/w), MDA-MB-361 (7000 c/w), HeLa (3000 c/w), FemX (4000 c/w), LS-174 (7000 c/w) and MRC-5 (5000 c/w) in culture medium and grown for 24 h. K562 (5000 c/w) cells were seeded 2 h before treatment. Stock solutions of investigated agents were made in DMSO at concentration of 10 mM, and afterward diluted with nutrient medium to desired final concentrations (in the range up to 100 μM). Cisplatin (CDDP) stock solution was made in 0.9% NaCl at concentration of 3.3 mM and afterward diluted with nutrient medium to desired final concentrations (in range up to 100 μM). Solutions of various concentrations of the examined compounds were added to the wells, except the control wells where only nutrient medium was added. All samples were done in triplicate. Nutrient medium with corresponding agent concentrations but without target cells, was used as a blank, also in triplicate.

Cells were incubated for 48 h with the test compounds at 37 °C, with 5% CO_2 in humidified atmosphere. After incubation, 20 μL of MTT solution, 5 mg/mL in phosphate buffer solution (PBS), pH 7.2, were added to each well. Samples were incubated for 4 h at 37 °C with 5% CO_2 in humidified atmosphere. Formazan crystals were dissolved in 100 μL of 10% sodium dodecyl sulfate (SDS). Absorbance was recorded on the ThermoLabsystems 408 Multiskan EX 200–240 V after 24 h at a wavelength of 570 nm. Concentration IC50 (μM) was defined as the concentration of drug producing 50% inhibition of cell survival. It is determined from the cell survival diagrams.

4.3.5. Cell cycle analysis

Flow-cytometric analysis of cell cycle phase distribution of HeLa cells, treated with investigated nickel complexes and cisplatin, as reference compound, was performed after staining fixed HeLa cells with propidium iodide (PI) [18].

HeLa cells were seeded at density of 2×10^5 cells/well at 6-well plate (NUNC) and growth in nutrition medium. After 24 h cells were continually exposed to investigated complexes with concentrations that correspond to 0.5× IC_{50}, IC_{50} and 1.5× IC_{50} (determined for 48 h treatment). After 48 h of continual treatment, cells were collected by trypsinization, washed twice with ice-cold PBS, and fixed for 30 min in 70% EtOH. After fixation, cells were washed again with PBS, and incubated with RNaseA (1 mg/mL) for 30 min at 37 °C. Cells were than stained with PI (400 μg/mL) 15 min before flow-cytometric analysis. Cell cycle phase distribution were

analyzed using a fluorescence activated sorting cells (FASC) Calibur Becton Dickinson flow cytometer and Cell Quest computer software.

4.3.6. DNA cleavage

Double-stranded closed circular high copy plasmid pUC19 (2686 base pairs with a molecular weight of 1.74×10^6 Da, isolated from *E. coli*) was purchased from Fermentas Life Sciences (EU). 0.5 μg of pUC19 in a 20 μL reaction mixtures in TS buffer (20 mM Tris/20 mM NaCl, pH 7.9), were incubated with different concentration of the complex at 37 °C for 1.5 h. The control sample was prepared with 3 μL of DMSO instead of the complex. The reaction mixtures were vortexed from time to time. The reaction was terminated by short centrifugation at 10,000 rpm and adding 7 μL of loading buffer (0.25% bromophenol blue, 0.25% xylene cyanol FF and 30% glycerol in TAE buffer, pH 8.24 (40 mM Tris–acetate, 1 mM EDTA)). The samples were subjected to electrophoresis on 1% agarose gel (Amersham Pharmacia-Biotech, Inc) prepared in TAE buffer pH 8.24. The electrophoresis was performed at a constant voltage (80 V) for 1.5 h (until bromophenol blue had passed through 75% of the gel). After electrophoresis, the gel was stained for 30 min by soaking it in an aqueous ethidium bromide solution (0.5 μg/mL), and after that was visualized under UV light.

Acknowledgments

Financial support of the Ministry of Education and Science of the Republic of Serbia (Grant OI 172055 and Grant III 41026).

Appendix A. Supplementary data

Supplementary data related to this article can be found at http://dx.doi.org/10.1016/j.ejmech.2013.07.039.

References

[1] M.J. McKeage, L. Maharaj, S.J. Berners-Price, Mechanisms of cytotoxicity and antitumor activity of gold(I) phosphine complexes: the possible role of mitochondria, Coord. Chem. Rev. 232 (2002) 127–135.
[2] J.F. González-Pantoja, M. Stern, A.A. Jarzecki, E. Royo, E. Robles-Escajeda, A. Varela-Ramírez, R.J. Aguilera, M. Contel, Titanocene–Phosphine derivatives as precursors to cytotoxic heterometallic $TiAu_2$ and TiM (M = Pd, Pt) compounds. Studies of their interactions with DNA, Inorg. Chem. 50 (2011) 11099–11110.
[3] M. Wenzel, B. Bertrand, M. Eymin, V. Comte, J.A. Harvey, P. Richard, M. Groessl, O. Zava, H. Amrouche, P.D. Harvey, P. Le Gendre, M. Picquet, A. Casini, Multinuclear cytotoxic metallodrugs: physicochemical characterization and biological properties of novel heteronuclear gold–titanium complexes, Inorg. Chem. 50 (2011) 9472–9480.
[4] R. Galassi, A. Burini, S. Ricci, M. Pellei, M. Rigobello, A. Citta, A. Dolmella, V. Gandinc, C. Marzano, Synthesis and characterization of azolate gold(I) phosphane complexes as thioredoxin reductase inhibiting antitumor agents, Dalton Trans. 41 (2012) 5307–5318.
[5] R. Starosta, A. Bykowska, M. Barys, A.K. Wieliczko, Z. Staroniewicz, M. Jeżowska-Bojczuk, Novel complexes of tris(aminomethyl)phosphanes with platinum(II): structural, spectroscopic, DFT and biological activity studies, Polyhedron 30 (2011) 2914–2921.
[6] A. Zanella, V. Gandin, M. Porchia, F. Refosco, F. Tisato, F. Sorrentino, G. Scutari, M. Rigobello, C. Marzano, Cytotoxicity in human cancer cells and mitochondrial dysfunction induced by a series of new copper(I) complexes containing tris(2-cyanoethyl)phosphines, Invest. New Drugs 29 (2011) 1213–1223.
[7] C. Santini, M. Pellei, G. Papini, B. Morresi, R. Galassi, S. Ricci, F. Tisato, M. Porchia, M. Rigobello, V. Gandin, C. Marzano, In vitro antitumour activity of water soluble Cu(I), Ag(I) and Au(I) complexes supported by hydrophilic alkyl phosphine ligands, J. Inorg. Biochem. 105 (2011) 232–240.
[8] V. Radulović, A. Bacchi, G. Pelizzi, D. Sladić, I. Brčeski, K. Andjelković, Synthesis, structure, and antimicrobial activity of complexes of Pt(II), Pd(II), and Ni(II) with the condensation product of 2-(diphenylphosphino)benzaldehyde and semioxamazide, Monatsh. Chem. 137 (2006) 681–691.
[9] N. Malešević, T. Srdić, S. Radulović, D. Sladić, V. Radulović, I. Brčeski, K. Anđelković, Synthesis and characterization of a novel Pd(II) complex with the condensation product of 2-(diphenylphosphino)benzaldehyde and ethyl hydrazinoacetate. Cytotoxic activity of the synthesized complex and related Pd(II) and Pt(II) complexes, J. Inorg. Biochem. 100 (2006) 1811–1818.
[10] M. Milenković, A. Bacchi, G. Cantoni, S. Radulović, N. Gligorijević, S. Aranđelović, D. Sladić, M. Vujčić, D. Mitić, K. Anđelković, Synthesis, characterisation and biological activity of Co(III) complex with the condensation product of 2-(diphenylphosphino)benzaldehyde and ethyl carbazate, Inorg. Chim. Acta 395 (2013) 33–43.
[11] R.A. de Souza, A. Stevanato, O. Treu-Filho, A.V.G. Netto, A.E. Mauro, E.E. Castellano, I.Z. Carlos, F.R. Pavan, C.Q.F. Leite, Antimycobacterial and antitumor activities of palladium(II) complexes containing isonicotinamide (isn): X-ray structure of trans-$[Pd(N_3)_2(isn)_2]$, Eur. J. Med. Chem. 45 (2010) 4863–4868.
[12] A. Bacchi, M. Carcelli, M. Costa, P. Pelagatti, C. Pelizzi, G. Pelizzi, Palladium(II) complexes containing a P, N-chelating ligand. Synthesis, characterization, and catalytic hydrogenation of double and triple bonds. X-ray structure of a phenyl ethynylpalladium(II) complex, Gazz. Chim. Ital. 124 (1994) 429–435.
[13] (a) A. Bacchi, M. Carcelli, M. Costa, A. Fochi, C. Monici, P. Pelagatti, C. Pelizzi, G. Pelizzi, L.M. Sanjuan Roca, Stable alkynyl palladium(II) and nickel(II) complexes with terdentate PNO and PNN hydrazone ligands, J. Organomet. Chem. 593–594 (2000) 180–191;
(b) P. Pelagatti, A. Bacchi, C. Bobbio, M. Carcelli, M. Costa, C. Pelizzi, C. Vivorio, Synthesis, characterization, and reactivity toward MeI of carbonyl Rh(I) complexes containing a PNO hydrazonic ligand, Organometallics 19 (2000) 5440–5446.
[14] (a) A. Bacchi, M. Carcelli, M. Costa, A. Leporati, E. Leporati, P. Pelagatti, C. Pelizzi, G. Pelizzi, Palladium(II) complexes containing a P, N chelating ligand Part II. Synthesis and characterisation of complexes with different hydrazinic ligands. Catalytic activity in the hydrogenation of double and triple C–C bonds, J. Organomet. Chem. 535 (1997) 107–120;
(b) P. Pelagatti, A. Bacchi, M. Carcelli, M. Costa, A. Fochi, P. Ghidini, E. Leporati, M. Masi, C. Pelizzi, G. Pelizzi, Palladium(II) complexes containing a P, N chelating ligand: part III. Influence of the basicity of tridentate hydrazonic ligands on the hydrogenating activity of unsaturated C–C bonds, J. Organomet. Chem. 583 (1999) 94–105.
[15] A. Bacchi, M. Carcelli, M. Costa, H.-W. Frühauf, K. Goubitz, P. Pelagatti, C. Pelizzi, M. Triclistri, K. Vrieze, Methyl and acetyl palladium(II) complexes containing a P, N, O tridentate hydrazone ligand, Eur. J. Inorg. Chem. 2002 (2002) 439–446.
[16] B.N. Meyer, N.R. Ferrigni, J.E. Putnam, L.B. Jacobsen, D.E. Nichols, J.L. McLaughlin, Brine shrimp: a convenient bioassay for active plant constituents, Planta Med. 45 (1982) 31–34.
[17] J.E. Anderson, C.M. Goetz, J.L. McLaughlin, M. Suffness, A blind comparison of simple benchtop-bioassays and human tumour cell cytotoxicities as antitumor prescreens, Phytochem. Anal. 2 (1991) 107–111.
[18] M.G. Ormerod, Analysis of DNA-general methods, in: M.G. Ormerod (Ed.), Flow Cytometry, a Practical Approach, Oxford University Press, New York, 1994, pp. 119–125.
[19] SAINT: SAX, Area Detector Integration, Siemens Analytical Instruments Inc., Madison, Wisconsin, USA G. Sheldrick, SADABS: Siemens Area Detector Absorption Correction Software, University of Goettingen, Germany, 1996.
[20] A. Altomare, M.C. Burla, M. Camalli, G. Cascarano, C. Giacovazzo, A. Guagliardi, A.G. Moliterni, G. Polidori, R. Spagna, Sir97: a New Program for Solving and Refining Crystal Structures, Istituto di Ricerca per lo Sviluppo di Metodologie Cristallografiche CNR, Bari, 1997.
[21] G. Sheldrick, Shelxl97, Program for Structure Refinement, University of Goettingen, Germany, 1997.
[22] (a) L.J. Farrugia, WinGX suite for small-molecule single-crystal crystallography, J. Appl. Crystallogr. 32 (1999) 837–838;
(b) M. Nardelli, PARST95 – an update to PARST: a system of Fortran routines for calculating molecular structure parameters from the results of crystal structure analyses, J. Appl. Crystallogr. 28 (1995) 659.
[23] (a) F.H. Allen, O. Kennard, R. Taylor, Systematic analysis of structural data as a research technique in organic chemistry, Acc. Chem. Res. 16 (1983) 146–153;
(b) I.J. Bruno, J.C. Cole, P.R. Edgington, M. Kessler, C.F. Macrae, P. McCabe, J. Pearson, R. Taylor, New software for searching the Cambridge Structural Database and visualizing crystal structures, Acta Crystallogr. B58 (2002) 389–397.
[24] Approved Standard M2-A6Performance Standards for Antibacterial Disk Susceptibility Test, sixth ed., NCCLS (National Committee for Clinical Laboratory Standards), Wayne, PA, 1997.
[25] P.A. Kethcum, Microbiology: Concept and Applications, John Wiley and Sons, New York, USA, 1988.
[26] R. Supino, Methods in molecular biology, in: S. O'Hare, C.K. Atterwill (Eds.), In Vitro Toxicity Testing Protocols, Humana Press, New Jersey, 1995, pp. 137–149.